ATTEMPTS TO DETERMINE ACOUSTIC ATTENUATION IN SEDIMENT DRAPES OVERLYING ROCKY SURFACES FROM SIDESCAN SONAR IMAGERY

N C Mitchell

University of Durham, Department of Geological Sciences, Durham, UK
& University of New Brunswick, Department of Surveying Engineering, Fredericton, Canada

1. INTRODUCTION

When studying geological structures on the sea floor, such as lava flows or rock debris, their age is a valuable clue to their origin. The amount of overlying fine-grained sediment is often used as a rough guide to geologic age. This presentation will discuss preliminary attempts to estimate the thicknesses of sediment drapes overlying rocky surfaces in 6.5 kHz GLORIA sidescan sonar imagery by inferring the amount of signal attenuation that has occurred in the sediment drape. First, the signal variation with grazing angle over a uniformly-buried surface, a lava flow, is analysed for attenuation, which is expected to increase towards shallow grazing angles and longer attenuating paths through the sediment layer. Second, a rocky surface is buried by varying amounts of sediment, which is analyzed at constant grazing angle. The rocky surface is produced by volcanoes at a midocean ridge spreading centre and the sediment thickens away from the centre at a rate which can be used to estimate the sediment accumulation rate.

2. ACOUSTIC MODEL

When mapping an area with sonars for the first time, complicated acoustical models have limited use for deriving information about the sea floor because there are usually insufficient data to constrain these models. In order to derive sediment information, therefore, an acoustic model must be simple. A first-order model for the attenuating effect of sediment drapes is illustrated in Figure 1.

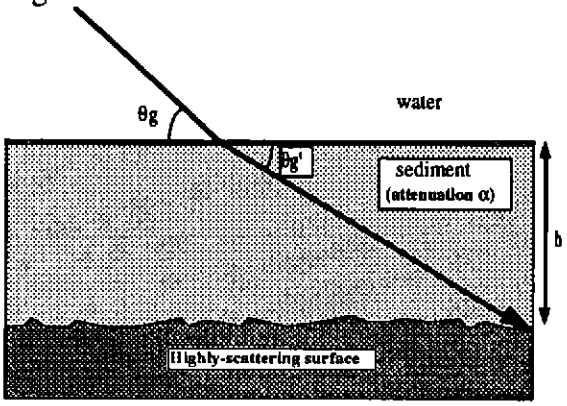

Figure 1. A simple acoustical model of rocky basement overlain by attenuating fine-grained sediments

A plane wave is incident upon a sea floor comprising a highly-backscattering surface overlain by fine-grained attenuating sediments. The sediment surface is flat so that the refracted wave is transmitted into the sediment as a plane wave. The intensity of the signal is reduced at the surface by the pressure transmission coefficient squared (T_{ws}^2), and is further reduced on the return path (by T_{sw}^2). Irregularities within the sediment are assumed to be small such that the plane wave is not broken up. The effective backscatter strength of the sedimented surface is

$$BS' = BS_v + 20 \log_{10}(T_{ws}T_{sw}) - \frac{2\alpha_{dB}h}{\sin(\theta_g')} \qquad (1),$$

the backscatter from the lava flow shows an anomalous 10 dB decrease with range from 4 to 20 km that is due to signal attenuation in the sediments overlying the flow. The difference of the two curves in Figure 3 is graphed against $1/\sin\theta_g$ in Figure 4, where the grazing angle θ_g was determined using ray-tracing. The difference in backscatter strength between the two curves in Figure 3, according to the first-order acoustical model in equation 1, is

$$\Delta BS = BS_v(\theta_g') - BS_s(\theta_g) + 20\log_{10}(T_{ws}T_{sw}) - \frac{2\alpha_{dB}h}{\sin(\theta_g')} \qquad (2),$$

where BS_V and BS_S are the effective surface backscatter strengths of the lava flow and "normal" sediments respectively. If the variation of T with angle is small, if the angular dependencies of BS_V and BS_S are sufficiently similar for the third term in equation 2 to dominate, if the sediment has constant thickness h, and if there is negligible refraction within the sediment, a graph of ΔBS against $1/\sin\theta_g$ will yield a straight line with slope $2h\alpha_{dB}$. Excluding data below 15° where refraction may be significant, the graph has a slope of -0.8 dB. Given that the sediment is 1-2 m thick [6], the data suggest a sediment attenuation coefficient of 0.2-0.4 dB/m, which compares favourably with other published attenuation values around 6.5 kHz.

4. MIDOCEAN RIDGES

Figure 5 shows a swath of GLORIA data collected across a midocean ridge. The brightness in the image decreases away from the spreading centre as the volcanic sea floor is progressively covered by sediments (the numbers below the image are kilometres measured from the spreading centre). To correct for the variable response of the GLORIA system, the data were first converted to relative sea floor backscatter strengths using the design characteristics of the sonar [7, 8]. Although the sonar is uncalibrated, this calculation is sufficient because this study involves only the variation and not absolute backscatter levels. The range is restricted to 5-10 km to avoid errors with the beam pattern calculation and effects of refraction in the sediments.

Sediment Thickness Distribution and Variability

Figure 6 shows the amplitude distributions for the areas outlined in Figure 5. The distributions are narrow over the ridge axis and widen as the sea floor becomes older. The centres of the distributions decrease, reflecting the steady overall accumulation of sediments. The upper -30 dB tail of the distributions remains at a level similar to that for the ridge axis ("young sea floor"), showing that abyssal hills are exposed by erosion or non-deposition on steeper slopes. Beyond 30 km from the spreading axis (~1 m.y), the lower tails of the distributions reach the -65 to -75 dB backscatter level of deep sediment ponds found on 10-m.y.-old sea floor [9] and the basement is probably masked by the sediment ponds in these areas (the level of backscatter from the sediments themselves exceeds the heavily attenuated backscatter from the basement). The changing shape of the distributions before 1 Ma (the distributions appear to smooth out from an initially narrow distribution over the spreading centre to broader distributions on older sea floor) can be explained relatively simply by noting that sediment accumulation is likely to be spatially-distributed because of sediment slumping or through the action of bottom currents so that different areas are left with varying amounts of sediment cover, leading to varying amounts of attenuation of the backscattered amplitudes. The smoothing of the distributions in Figure 6 can therefore be interpreted as a convolution of the bare rock amplitude

distribution by the varying amounts of attenuation.

Equation 1 can be used to express this interpretation mathematically using probability density functions (PDFs). The sediments are assumed to accumulate in such a way that there is no statistical connection between the backscatter strength of the basement and the attenuation due to the sediments, and these may be treated as independent random variables. The backscatter strength distribution, which is represented by the PDF $p_{bs'}(A)$, is then given by a convolution [10] of a PDF representing the variations in backscatter strength of the basement surface $p_{bs}(A)$ with a PDF representing the variations in the amount of attenuation $p(H)$, where $H=h2\alpha_{dB}/\sin\theta_g'$ and A is the amplitude in decibels.

$$p_{bs'}(A) = p_{bs}(A) * p(-H) \qquad (3).$$

The asterisk represents the convolution operator. Transmission of the signal through the sediment surface is common to areas of both thick and thin sediment cover, and therefore the transmission coefficient is constant and is left out of the convolution. The parameter in the attenuation PDF is negative due to the definition of H. The amplitudes are further varied because of interference effects which cause image speckle and other fluctuations caused by the sonar system. Since the sonar system's effective gain and the sea floor's backscatter strength are additive independent random variables, the distribution of backscatter strengths measured by the sonar is given by a further convolution with a PDF $p_u(A)$ representing these variations [11].

$$p_m(A) = (p_{bs} * p_u) * p(-H) \qquad (4).$$

The progressive broadening of the distributions in Figure 6 is therefore due to a convolution of the backscatter distribution of the volcanic basement ($p_{bs}*p_u$) with a sediment attenuation distribution $p(H)$, which represents an increasing range of sediment thickness as the sea floor ages. Furthermore, if the distribution of amplitudes measured over the spreading centre represents the PDF $p_{bs}*p_u$ for the more sedimented areas, the PDF $p(H)$ may be recovered by deconvolving the distributions using the spreading centre distribution as the response function. The distributions of sediment thickness $p(h)$ are then given by rescaling $p(H)$ and parameter H with an estimate of the factor $2\alpha_{dB}/\sin\theta_g'$. This is presented separately [5] and suggests that it may be possible to determine sediment thicknesses as great as 10-20 m with 6.5 kHz sonar.

Sediment Accumulation Rate

The means of the signal levels in Figure 6 and two further data sets are shown in Figure 7. The graphs are linear between 5 and 30 km, which implies a steady increase in the average sediment thickness. The graphs are non-linear within 5 km of the spreading axis, presumably where there are active geological processes such as faulting and volcanism over the valley floor. Beyond about 30 km, the flattening of the curves is due to sediments accumulating at discrete sites (sediment ponds) which acoustically mask the underlying basement and these slowly grow in area while the remainder of the sea floor maintains a relatively uniform range of sediment thickness. We can describe the linear part of the graphs mathematically by taking the mean of equation 1. We assume that BS and h are independent, that α_{dB} and $\mathrm{cosec}(\theta_g')$ are constant, and that the mean backscatter strength of the basement is constant with distance from the spreading centre. The slopes of these graphs are

$$\frac{d<BS'>}{dx} = \frac{2\alpha_{dB}S}{R\sin(\theta_g')} \quad dB/km \qquad (5),$$

where R is the sea floor half-spreading rate in km/m.y. (3 km/m.y. here), which can be estimated by modelling sea floor magnetic anomalies. This equation can be solved for the sediment accumulation rate S (mm/ka). Assuming an attenuation coefficient of 0.3 dB/m, the ~0.34 dB/km average slope of Figure 7 suggests an average sediment accumulation rate of ~6 mm/ka.

5. DISCUSSION

Clearly, when mapping sediment drapes for academic or offshore engineering applications, the most desireable tool is a sub-bottom profiler. Why then bother with indirect sonar methods such as this? There are three possible uses: the method can potentially determine sediment thicknesses that are unresolvable with sub-bottom profilers, a sidescan sonar's spatial coverage can be used to fill between lines in those cases where sub-bottom profilers can resolve sediments, and where the sea floor's topography is rough, such as over midocean ridges, scattering from the abyssal hills obscures the sediments in sub-bottom profiler records but sidescan sonar can still detect these sediment thicknesses (this is evident from Figure 7). However, there are problems with the sonar method. In addition to the uncertainty in attenuation coefficients, the spatial resolution of sidescan sonar causes a bias because the amount of attenuation depends on the variability of the sediment thickness over spatial scales finer than the sonar footprint; a given volume of sediment will reduce the backscattered amplitudes more if it drapes on the topography than if it fills low areas in the basement. Model results [5] show that sediment thicknesses may be underestimated and sedimentation rates may also be too low. This source of error will need further empirical investigation.

As a method for mapping sediment accumulation rates over ridges, this is important because the sediments are carbonaceous and their accumulation represents a sink of carbon in the oceans, with implications for the overall carbon cycle [12]. Accumulation rates can be measured from individual sediment cores but these are unreliable because sediment erosion and redeposition are difficult to account for. Rates can be determined from sub-bottom profiler records by mapping the rate of thickening of sediments away from ridges but, to avoid the effect of abyssal-hill scattering, the profiler must be towed near the sea floor [13, 14]. The advantages of sidescan sonar methods are that they average out the sediment thickness variations that affect cores and they are collected efficiently. Probably a combined approach, using sonar data but with deep-tow records for calibration, will be the most practical way to map variations in sedimentation rates along ridges, which can then be compared with variations in biological productivity.

6. CONCLUSIONS

A preliminary assessment has been made of a simple acoustical model for a highly scattering geological surface covered by sediments, in which the attenuation of the backscattered signal is proportional to the sediment thickness and to the sediment attenuation coefficient. The amplitude variation with range for a GLORIA 6.5 kHz sidescan sonar image of a lava sheet flow is consistent with an attenuation coefficient of 0.2-0.4 dB/m for the overlying fine-grained sediments. The result suggests that preliminary estimates of sediment drapes from sidescan

sonar data may be possible.

Over the South East Indian Ridge, the mean signal level decreases in GLORIA data collected with the sonar towed away from a spreading centre. When interpreted with the simple model, this suggests that the average rate of sediment accumulation is ~6 mm/ka (assuming the attenuation coefficient is 0.3 dB/m). Furthermore, the amplitude distribution of the sonar may also be used to recover information on the variability of sediment thickness via a simple convolution model.

Acknowledgement Robin Holcomb of the US Geological Survey and Lindsay Parson of the IOSDL are gratefully acknowledged for the GLORIA data used in this study. This work has been supported by Research Fellowships from the Royal Commission for the Exhibition of 1851, the NERC and the NSERC of Canada.

7. REFERENCES

[1] L BREKHOVSKIKH & Y LYSANOV, 'Fundamentals of Ocean Acoustics', 1982, New York: Springer

[2] E L HAMILTON & R T BACHMAN, 'Sound velocity and related properties of marine sediments', J. Acoust. Soc. Am., 72 p1891-1904 (1982)

[3] E L HAMILTON, 'Geoacoustic modeling of the sea floor', J. Acoust. Soc. Am., 68 p1313-1340 (1980)

[4] A C KIBBLEWHITE, 'Attenuation of sound in marine sediments: A review with emphasis on new low-frequency data', J. Acoust. Soc. Am., 86 p716-738 (1989)

[5] N C MITCHELL, 'A model for attenuation of backscatter due to sediment accumulations and its application to determine sediment thickness with GLORIA sidescan sonar', J. Geophys. Res., in review (1993)

[6] D A CLAGUE, R T HOLCOMB, J M SINTON, R S DETRICK & M E TORRESAN, 'Pliocene and Pleistocene alkalic flood basalts on the seafloor north of the Hawaiian islands', Earth Planet. Sci. Lett., 98 p175-191 (1990)

[7] N C MITCHELL & M L SOMERS, 'Quantitative backscatter measurements with a long range side-scan sonar', IEEE J. Oceanic Eng., 14 p368-374 (1989)

[8] N C MITCHELL, 'Improving GLORIA images using Sea Beam data', J. Geophys. Res., 96 p337-351 (1991)

[9] N C MITCHELL, 'Investigation of the structure and evolution of the Indian Ocean Triple Junction using GLORIA and other geophysical techniques', 1989, D. Phil. thesis, Oxford University, England

[10] W S BURDIC, 'Underwater acoustic system analysis', 1991, London: Prentice-Hall

[11] F T ULABY, T R HADDOCK & R T AUSTIN, 'Fluctuation statistics of millimeter-wave scattering from distributed targets', IEEE Trans. Geosci. Remote Sens., 26 p268-281 (1988)

[12] W S BROECKER & T-H PENG, 'Tracers in the Sea', 1982, Palisades, New York: Lamont-Doherty Geological Observatory, Columbia University

[13] K D KLITGORD & J D MUDIE, 'The Galapagos spreading centre: a near-bottom geophysical survey', Geophys. J. R. astr. Soc., 38 p563-586 (1974)

[14] P LONSDALE, 'Structural geomorphology of a fast-spreading rise crest: the East Pacific Rise near 3° 25'S', Mar. Geophys. Res., 3 p251-293 (1977)

REMOTE-SENSING SEDIMENTS OVERLYING ROCKY SURFACES

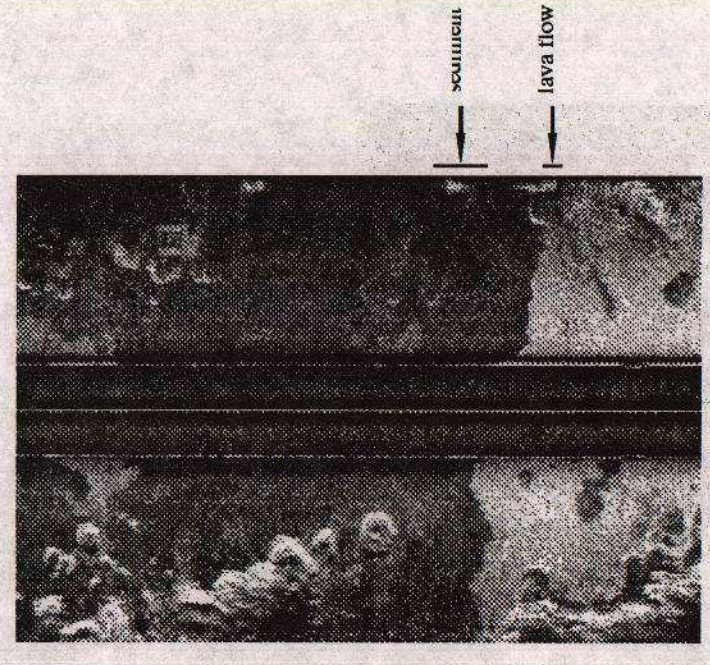

Figure 2. A GLORIA swath crossing a lava flow 100 km north of the Hawaiian islands. High backscattered amplitudes are represented by light grey. The lava shows up clearly despite being buried by 1-2 m of fine-grained sediment.

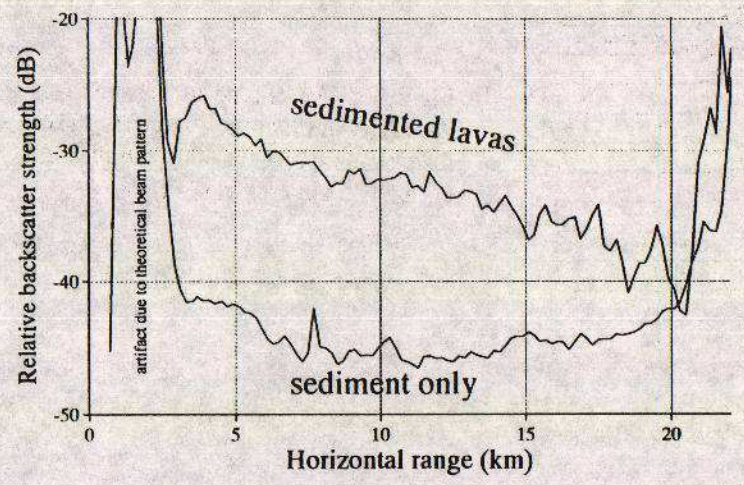

Figure 3. Two cross-sections indicated Figure 2. Amplitudes were averaged within 200 m bins in range and over (sediments) 50 and (sedimented lava) 20 scans. The backscattered amplitudes from the lava anomalously decrease by 10 dB over the swath compared to the reference "normal" sediments because of attenuation in the 1-2 m of sediments overlying the lava.

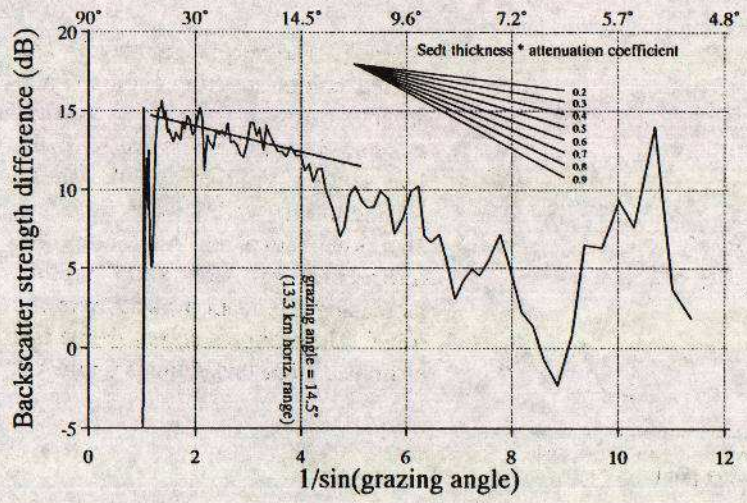

Figure 4. The difference in signal strength between the lavas and the "normal" sediments (Figure 3), which emphasizes the effect of attenuation in the sediments overlying the lava. The straight line through the data indicates an attenuation rate of ~0.2-0.4 dB/m in these overlying sediments.

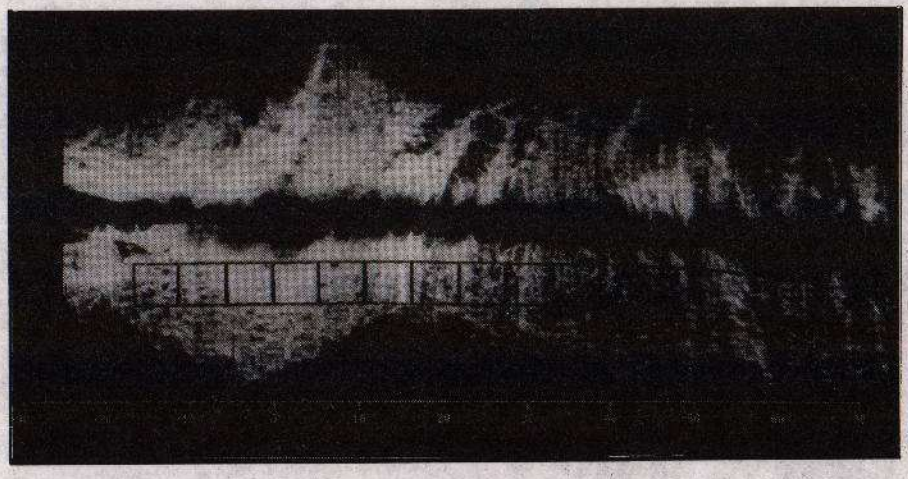

Figure 5. A swath of GLORIA data across a spreading centre in the central Indian Ocean. High amplitudes are plotted white.

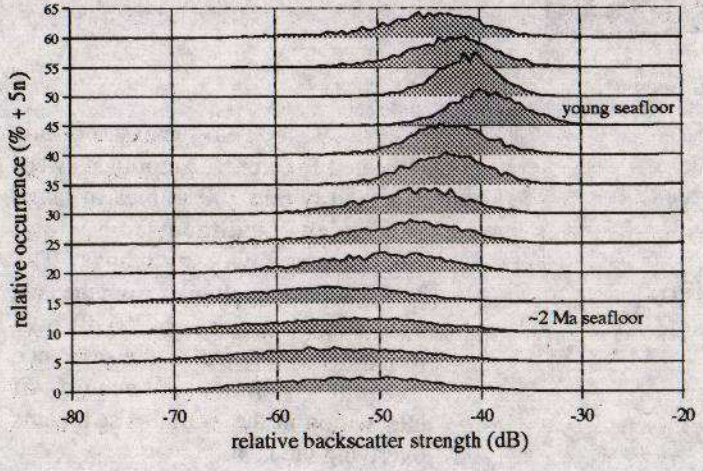

Figure 6. Amplitude histograms for the areas outlined in Figure 5. The histograms represent 4000 samples in each 5 X 5 km area of sea floor.

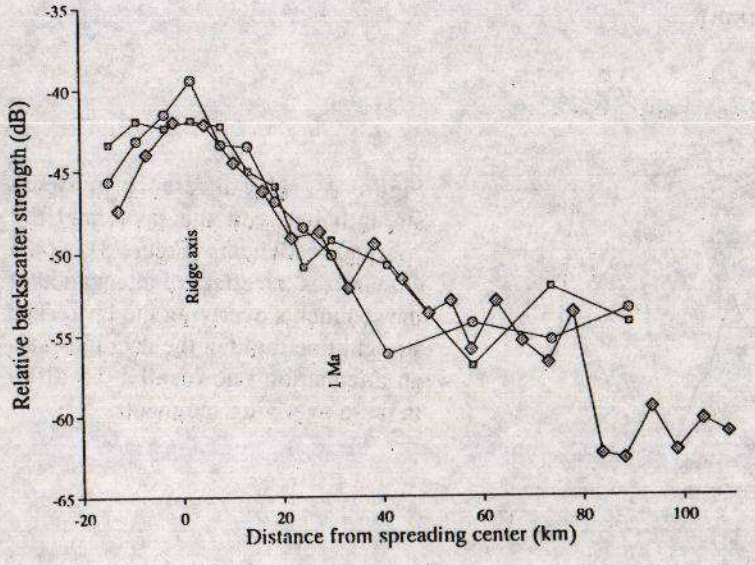

Figure 7. The mean signal level. The circled points are from Figure 6 and other symbols from two further swaths. Standard errors are ~0.1 dB. The simple gradient of the mean outside the rift valley walls from 5 to 30 km implies a constant sedimentation rate and steadily increasing attenuation away from the ridge. The sediment accumulation rate estimated from this slope is 6 mm/ka.